Resistance of Akt kinases to dephosphorylation through ATP-dependent conformational plasticity

Tung O. Chan[a,b,1,2], Jin Zhang[a,1], Ulrich Rodeck[b,c,d], John M. Pascal[b,e], Roger S. Armen[f], Maureen Spring[a], Calin D. Dumitru[b,3], Valerie Myers[a], Xue Li[a], Joseph Y. Cheung[a], and Arthur M. Feldman[a,4]

[a]Center for Translational Medicine, Department of Medicine; [c]Department of Dermatology and Cutaneous Biology; [e]Department of Molecular Biology and Biochemistry; [d]Department of Radiation Oncology; [f]Department of Pharmaceutical Sciences, School of Pharmacy; and [b]Kimmel Cancer Center, Thomas Jefferson University, Philadelphia, PA 19107

Edited by John Kuriyan, University of California, Berkeley, CA, and approved September 19, 2011 (received for review June 20, 2011)

Phosphorylation of a threonine residue (T308 in Akt1) in the activation loop of Akt kinases is a prerequisite for deregulated Akt activity frequently observed in neoplasia. Akt phosphorylation in vivo is balanced by the opposite activities of kinases and phosphatases. Here we describe that targeting Akt kinase to the cell membrane markedly reduced sensitivity of phosphorylated Akt to dephosphorylation by protein phosphatase 2A. This effect was amplified by occupancy of the ATP binding pocket by either ATP or ATP-competitive inhibitors. Mutational analysis revealed that R273 in Akt1 and the corresponding R274 in Akt2 are essential for shielding T308 in the activation loop against dephosphorylation. Thus, occupancy of the nucleotide binding pocket of Akt kinases enables intramolecular interactions that restrict phosphatase access and sustain Akt phosphorylation. This mechanism provides an explanation for the "paradoxical" Akt hyperphosphorylation induced by ATP-competitive inhibitor, A-443654. The lack of phosphatase resistance further contributes insight into the mechanism by which the human Akt2 R274H missense mutation may cause autosomal-dominant diabetes mellitus.

protein kinase B | inhibitors hijacking kinase activation | kinase priming phosphorylations | PP2A

The serine/threonine Akt protein kinases (Akt1, Akt2, and Akt3) affect multiple cellular functions related to cell growth and survival, differentiation, metabolism, and migration (reviewed in refs. 1, 2). Essential functions of Akt kinases in mammalian physiology are highlighted by retarded growth and increased neonatal mortality in Akt1 knockout mice, severe diabetes in Akt2 knockout mice, and reduced brain size in Akt3 knockout animals (reviewed in ref. 3). Furthermore, an inherited inactivating mutation in Akt2-R274 has been linked to autosomal-dominant severe insulin resistance and diabetes mellitus in humans (4).

The activation state of Akt is regulated by controlling phosphorylation of two regulatory residues in its centrally located activation loop (T308 in Akt1) and in the carboxyl-terminal tail (S473 in Akt1) by two separate kinases (PDK1 and PDK2) (reviewed in refs. 1, 2). Phosphorylation of these regulatory sites is enabled by conformational changes induced by docking of the Akt pleckstrin homology (PH) domain to the membrane lipid products, PtdIns(3,4,5)P_3 or PtdIns(3,4)P_2. PDK-dependent Akt1 phosphorylation is reversed by the abundantly expressed protein phosphatase 2A (PP2A) which dephosphorylates pT308 and, to a lesser extent, pS473 (5, 6). Specifically, Akt has been identified as the substrate of a complex containing the regulatory B55α or B56β subunits of PP2A in *Caenorhabditis elegans*, *Drosophila melanogaster*, and in mammalian cells (7–9). The functional relevance of B56β-containing PP2A to Akt regulation is further underscored by genetic studies in *C. elegans* demonstrating modulation of insulin/insulin-like growth factor effects on longevity, fat metabolism, and stress resistance by this phosphatase (9).

Hyperactivation and phosphorylation of Akt kinases is commonly observed in diverse tumor types and has motivated the development of pharmacological Akt inhibitors (10). A non-ATP-competitive allosteric Akt inhibitor, AKT inhibitor VIII (also termed Akt-I 1/2), prevents Akt phosphorylation (11, 12). The Akt1:Inhibitor VIII crystal structure and Forster resonance energy transfer-based in vivo dynamics experiments show that inhibitor VIII binding stabilizes an inactive Akt conformation that prevents ATP binding to the kinase (13, 14). Another class of Akt inhibitors competes with ATP for binding to the ATP acceptor site in the catalytic Akt1 domain; these include A-443654 (15) and GSK690693 (16). Interestingly, inhibition of Akt kinase activity by these ATP-competitive agents in cells and in animals is associated with hyperphosphorylation of the Akt regulatory residues, T308 and S473. This inhibitor-induced "paradoxical" Akt hyperphosphorylation is not due to enhancement of upstream signals to compensate for Akt signal loss but rather is related to occupation of Akt nucleotide-binding pocket by these inhibitors (17). It is not clear how inhibitor occupation of nucleotide-binding pocket by Akt inhibitors triggers Akt hyperphosphorylation, while allosteric agents binding outside the nucleotide-binding pocket inhibit Akt phosphorylation.

Here, we describe a molecular mechanism regulating the phosphorylation state of Akt kinases that depend on subcellular location and on occupancy of the ATP binding pocket. Specifically, we demonstrate that recruitment of Akt1 to the plasma membrane confers resistance to dephosphorylation of pT308 and this resistance further depends on ATP acceptor site occupancy by ATP or ATP-competitive inhibitors. In vitro, binding of either ATP or ATP-competitive inhibitors rendered Akt1 phospho-T308 highly resistant to dephosphorylation by the PP2A phosphatase. We propose that ATP occupancy facilitates intramolecular interactions of phosphorylated T308 with two residues in the Akt1 catalytic cleft (R273, H194) that restrict phosphatase access. This mechanism provides an explanation for Akt hyperphosphorylation induced by ATP-competitive but not allosteric Akt inhibitors. Disrupting these interactions by mutation obviates phosphatase resistance of pT308 and enables rapid dephosphorylation. Mutation of the homologous site in Akt2 (R274H), known to cause

Author contributions: T.O.C., J.Z., U.R., R.S.A., and C.D.D. designed research; T.O.C., J.Z., J.M.P., R.S.A., M.S., V.M., and X.L. performed research; T.O.C. and J.Z. contributed new reagents/analytic tools; T.O.C., J.Z., R.S.A., C.D.D., J.Y.C., and A.M.F. analyzed data; and T.O.C., U.R., J.M.P., J.Y.C., and A.M.F. wrote the paper.

The authors declare no conflict of interest.

This article is a PNAS Direct Submission.

[1]T.O.C. and J.Z. contributed equally to this work.

[2]To whom correspondence should be addressed. E-mail: tung.chan@KimmelCancerCenter.org.

[3]Present address: Merck Research Laboratories, West Point, PA 19486.

[4]Present address: Temple University School of Medicine, Philadelphia, PA 19140.

See Author Summary on page 18581.

This article contains supporting information online at www.pnas.org/lookup/suppl/doi:10.1073/pnas.1109879108/-/DCSupplemental.

autosomal-dominant insulin resistance in humans (4), also obviates ATP-induced phosphatase resistance at the Akt2 T309 site.

Results

ATP Occupancy Regulates T308 Dephosphorylation of Membrane-Localized Akt1. Binding to D3-phosphorylated phosphoinositide lipids anchors the Akt1 protein kinase at cell membranes, enables activation loop phosphorylation (T308 in Akt1), and induces Akt kinase activity. Similarly, targeting Akt1 to the cell membrane with a fusion protein consisting of Akt1 and myristoylation signal (MyrAkt1) was associated with "constitutive" T308 phosphorylation in H9C2 myoblasts as it occurred in culture medium lacking exogenous growth factors (Fig. 1*A*). Adding an allosteric inhibitor of the Akt kinase (Inhibitor VIII) to these cells led to MyrAkt1 dephosphorylation (>90%) within 30 min and dephosphorylation was inhibited by phosphatase inhibitors, calyculin or okadaic acid (Fig. 1*B*). Furthermore, the ATP-competitive Akt inhibitor, A-443654, prevented Inhibitor-VIII-induced Akt dephosphorylation even more effectively than the phosphatase inhibitors.

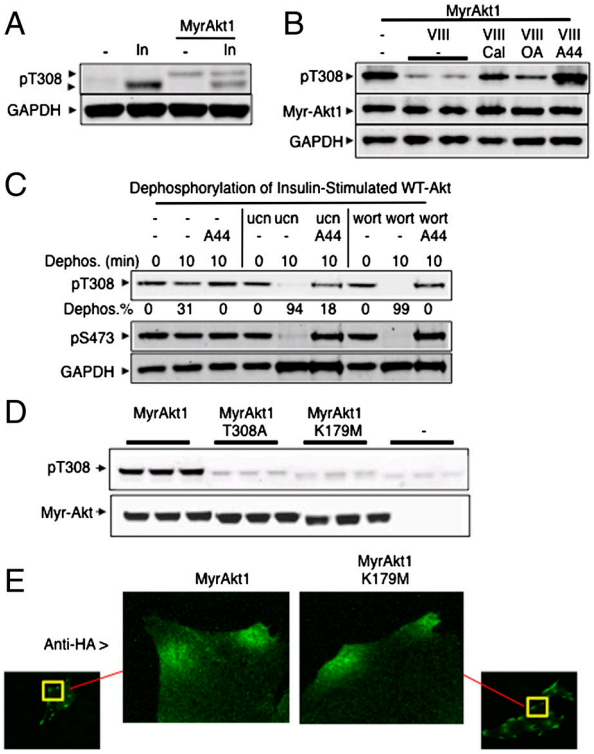

Fig. 1. ATP binding site occupancy regulates Akt1 dephosphorylation. (*A*) H9C2 cells transfected with HA-tagged MyrAkt1 were incubated for 4 h in medium free of exogenous growth factors before adding 1 ug/mL insulin for 30 min. Protein extracts were subjected to immunoblot analysis using antibodies to phospho-Akt T308 and GAPDH. (*B*) MyrAkt1 expressing H9C2 cells were incubated in growth factor-free medium with 10 uM VIII (allosteric Akt inhibitor) in the presence or absence of 10 uM A-443654, 100 nM calyculin or 2.5 uM okadaic acid for 30 min. Protein extracts were subjected to immunoblot analysis using phospho-Akt T308 antibody. (*C*) H9C2 cells grown in exogenous growth factor-free medium were stimulated with 1 ug/mL insulin for 20 min followed by 10 min in growth factor-free media supplemented with 10 uM A-443654, 200 nM wortmannin (PI-3 kinase inhibitor) or 0.5 uM UCN01 (PDK1 inhibitor) as indicated. Levels of Akt phosphorylation on T308 and S473, total Akt and GAPDH were determined by immunoblotting. Quantification shows percentage of Akt dephosphorylation (Dephos. %). (*D*) MyrAkt1 was mutated to ablate either ATP binding (K179M) or T308 phosphorylation (T308A). MyrAkt1 and mutants were transiently expressed in H9C2 cells for 48 h followed by immunoblot analysis of Akt T308 phosphorylation and HA-tag expression. (*E*) K179M mutation did not alter intracellular MyrAkt1 localization. H9C2 cells expressing MyrAkt1-HA and K179M mutant were fixed and stained. Immunofluorescence staining of cells with anti-HA-tag antibody (green). 60X whole cell images (small) and enlarged portion of the yellow square image are shown.

To determine whether A-443654 also inhibited dephosphorylation of wild-type (WT)-Akt1, H9C2 cells were stimulated with insulin for 20 min to induce endogenous Akt phosphorylation. To effect Akt dephosphorylation, cells were then incubated in growth factor-free medium with and without the PDK1 inhibitor, UCN01, or the PI-3 kinase inhibitor, wortmannin. Under these conditions, A-443654 delayed Akt dephoshorylation at both T308 and S473 sites (Fig. 1*C*). We further observed that, in growth factor-starved conditions, A-443654 treatment alone only weakly induced Akt1 phosphorylation, yet A-443654 potently synergized with insulin to induce Akt1 hyperphosphorylation at T308 (Fig. S1*A*). These results are consistent with the hypothesis that A-443654 induces Akt hyperphosphorylation by inhibiting Akt dephosphorylation.

The three-dimensional structures of Akt kinase complexed with Inhibitor VIII showed that Inhibitor VIII may restrict access of ATP to the Akt kinase domain by stabilizing interactions between the PH domain and kinase domain (14). In contrast, A-443654, as an ATP-competitive inhibitor, binds to the ATP binding pocket itself with high affinity (18). To test whether occupation of ATP binding pocket regulates Akt T308 dephosphorylation, we mutated the ATP binding lysine residue in MyrAkt1 to methionine (K179M). As controls, we also generated mutants that abolished the phosphorylation target in the activation loop (T308A). Upon transfection into H9C2 cells, the K179M-MyrAkt1 mutant exhibited reduced steady-state T308 phosphorylation to a level similar to the T308A mutant (Fig. 1*D*). Confocal microscopy (Fig. 1*E*) and membrane fractionation (Fig. S1*B*) confirmed that K179M mutation did not alter MyrAkt1 subcellular localization. Collectively, these pharmacological and genetic data support the model that the occupancy of the ATP acceptor site in Akt kinase affects the kinetics of T308 dephosphorylation.

Occupation of ATP Acceptor Site by ATP and Its Analogs Resists T308 Dephosphorylation In Vitro. Next we determined whether occupation of the ATP acceptor site regulated T308 dephosphorylation in cell extracts. To this end, constitutively phosphorylated MyrAkt1 was expressed in Hela cells followed by rapid dry-ice freezing/extraction. Upon further incubation of cell extracts at 30 °C, MyrAkt1 was dephosphorylated within 15 min and both, calyculin and the A-443654 Akt inhibitor independently blocked T308 dephosphorylation (Fig. 2*A*). However, unlike calyculin, A-443654 inhibited Akt1 dephosphorylation but not dephosphorylation of GSK-β, PRAS40, or ERK1/2 (Fig. 2*A*, Fig. S2*A*). Thus, in cell extracts devoid of kinase activity due to the presence of EDTA, A-443654 specifically inhibited dephosphorylation of MyrAkt1. This effect of A-443654 extended to constitutive phosphorylated WT-Akt in per-vanadate-treated Hela cell extracts (Fig. S2*B*). and in insulin-treated H9C2 cell extracts (Fig. S2*C*).

Membrane-associated Akt is dephosphorylated primarily by the type 2A serine/threonine phosphatase (PP2A) (5, 6). To assess whether A-443654 inhibits Akt1 dephosphorylation by PP2A in vitro, we incubated purified PP2A catalytic subunit (PP2A-C) with immunoprecipitated phosphorylated MyrAkt1 in a solution containing sonicated phosphatidylserine and phosphatidylcholine micelles. Under these conditions, PP2A-C efficiently dephosphorylated phospho-MyrAkt1 by 90% within 30 min, and 20 uM A-443654 almost completely counteracted this effect (Fig. 2*B*). As expected, ATP similarly inhibited MyrAkt1 dephosphorylation, although at a concentration (1 mM) considerably higher than that of A-443654 required for this effect (Fig. S3*A*). Considering that active Akt kinase would rapidly hydrolyse and turnover ATP occupying its acceptor site, we assessed whether blocking Akt ATP hydrolysis with a high affinity pseudosubstrate peptide inhibitor (I-T15A, VELDPEFEPRARERAYAFGH) could lower

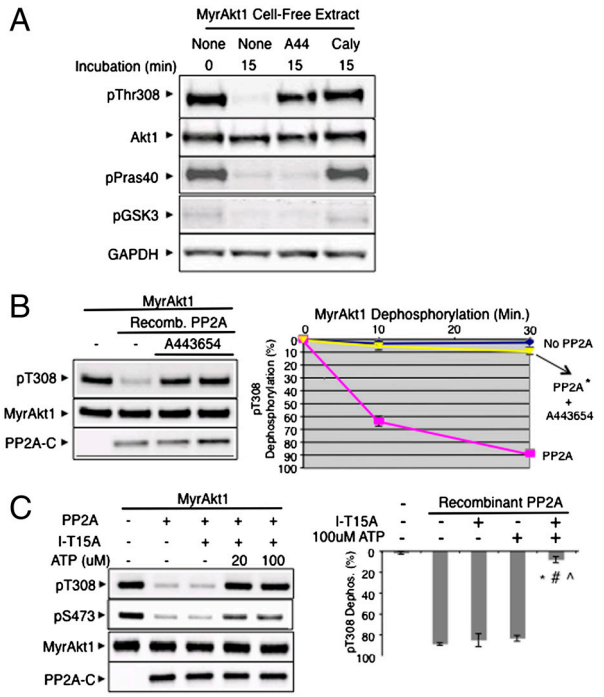

Fig. 2. A443654 or ATP binding inhibits Akt dephosphorylation. (*A*) A443654 inhibits MyrAkt1 dephosphorylation in cell extracts. MyrAkt1 expressing Hela cells were flash-frozen and extracted in ice. Aliquots of cell extracts were treated with A443654 or calyculin on ice before incubation at 30 °C for 15 min. After incubation, protein extracts were subjected to immunoblot analysis using antibodies detecting phosphorylated Akt (T308), GSK3β (S9), and Pras40 (T246) and GAPDH. (*B*) A443654 inhibits recombinant PP2A-mediated Akt dephosphorylation. Immunoprecipitated MyrAkt1 was incubated with recombinant PP2A (40 ng PP2A-C) for 30 min, 30 °C in the presence of A443654 (2–20 uM). Images show MyrAkt1 T308 phosphorylation, HA-tagged MyrAkt1 and PP2A-C expression. Graph shows the percentage pT308 dephosphorylation. $*P < 0.001$ for PP2A vs. PP2A+A44 at 30 min. (*C*) ATP inhibits recombinant PP2A-mediated Akt dephosphorylation in the presence of Akt-specific pseudosubstrate peptide (I-T15A). Immunoprecipitated MyrAkt1 was incubated with recombinant PP2A for 30 min, 30 °C in a buffer containing 5 mM MgCl2, 400 uM sonicated lipid micelles, 25 uM high affinity Akt pseudosubstrate inhibitor (I-T15A) and increasing concentrations of ATP (0, 20 uM or 100 uM) as indicated. Immunoblot images show MyrAkt1 T308 and S473 phosphorylation, HA-tagged MyrAkt1 and PP2A-C expression. Graph shows the percentage pT308 dephosphorylation in the presence PP2A alone ($n = 11$), PP2A with 100 uM ATP ($n = 8$), with 25 uM I-T15A peptide ($n = 3$) or both ($n = 7$). $*P < 0.001$ vs. PP2A, $\#P < 0.05$ vs. PP2A/ATP, $\wedge P < 0.05$ vs. PP2A/I-15A (Nonparametric ANOVA, Kruskal-Wallis).

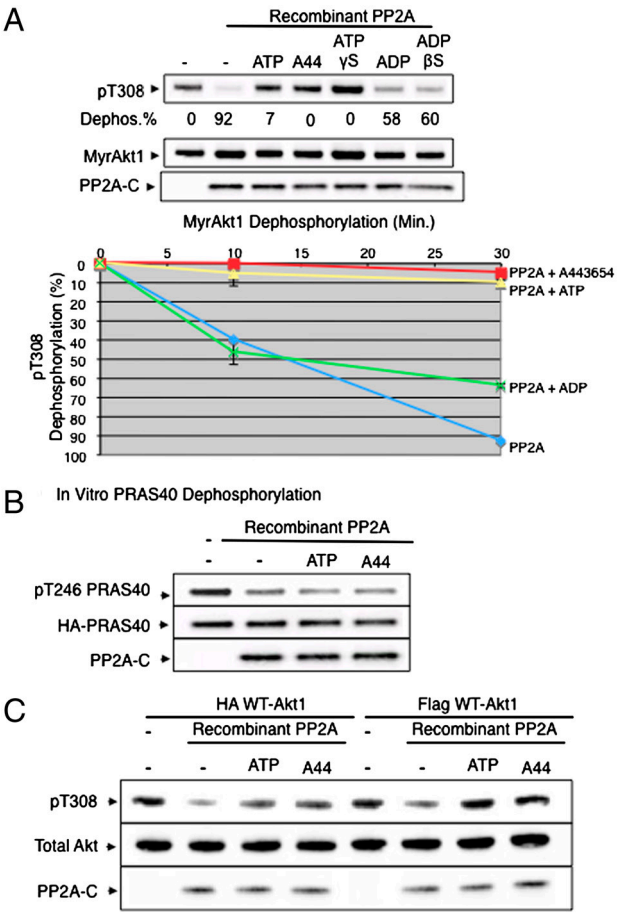

Fig. 3. Differential regulation of Akt dephosphorylation by different nucleotides. (*A*) Effects of ATP and ADP analogs on MyrAkt1 dephoshorylation. Immuno-purified MyrAkt1 was incubated with recombinant PP2A, 25 uM I-T15A inhibitor peptide and as indicated, 100 uM ATP, 20 uM A-443654, 100 uM ATPγS, 100 uM ADP or 100 uM ADPβS. Akt expression and phosphorylation and PP2A-C expression were analyzed by immunoblotting. Quantification shows the percentage of decrease in pT308 phosphorylation (Dephos. %) relative to untreated control after 30 min at 30 °C. (*B*) ATP or A443654 do not inhibit phospho-PRAS40 dephosphorylation. Hela cells expressing HA-tagged PRAS40 were stimulated with 100 uM Per-VO4 for 15 min to induce phosphorylation. Immunopreciptated phospho-PRAS40 was incubated with recombinant PP2A with 100 uM ATP/25 uM I-T15A peptide or 20 uM A-443654 as indicated. PRAS40 phosphorylation (Thr246), total PRAS40, and PP2A-C expression were analyzed by immunoblotting. (*C*) ATP and A443654 inhibit WT Akt1 dephosphorylation. HA-tagged WT-Akt1 or Flag-Tagged WT-Akt were prephosphorylated with 100 uM Per-VO4 stimulation and immunoprecipitated with anti-Flag beads or ant-HA beads. Phospho-WT-Akt was incubated with recombinant PP2A in the presence of 100 uM ATP or 10 uM A-443654 as indicated. T308 phosphorylation, total Akt1 and PP2A-C expression were analyzed by immunoblotting.

the ATP concentration required to inhibit Akt dephoshorylation. Consistent with this notion, I-T15A reduced the ATP concentration needed to inhibit both T308 and S473 dephosphorylaiton from 1 mM to 20 uM (Fig. 2*C*). Collectively, these data suggested that sustained occupation of ATP acceptor site with either ATP or an ATP-competitive inhibitor renders phosphorylated Akt highly resistant to PP2A-mediated dephosphorylation.

ATP and Analogs Inhibit Akt1 Dephosphorylation by Binding to Akt Kinase. To determine the specificity of ATP acceptor site occupancy for dephosphorylation resistance, we tested the effects of several other ATP-derivatives on MyrAkt1 dephosphorylation. ATP, ATP-γS, and A-443654 significantly reduced Akt dephosphorylation in the presence of I-T15A pseudosubstrate peptide (Fig. 3*A*). On the other hand, ADP and ADP-βS were markedly less effective in blocking dephosphorylation at both 10 min and 30 min incubation time points (Fig. 3*A*).

To rule out that ATP or A-443654 directly inhibited PP2A catalytic activity, we determined the effects ATP and A-443654 on PP2A-dependent dephosphorylation of a target unrelated to Akt, phospho-PRAS40. Under conditions identical to those used in the Akt dephosphorylation assay, neither ATP nor A-443654 affected the ability of PP2A to dephosphorylate PRAS40 (Fig. 3*B*). Finally, to determine whether WT-Akt similarly resisted PP2A-C dephoshorylation in vitro, we immunoprecipitated prephosphorylated HA-tagged or Flag-tagged WT-Akt1 from Hela cells. Fig. 3*C* shows that both HA-tagged and Flag-tagged phospho-WT-Akt1 resisted PP2A-C dephosphorylation in the presence of ATP or A-443654. Collectively, these data suggest that ATP inhibited Akt1 dephosphorylation, not by inhibiting PP2A activity, but by binding to Akt kinase.

Phosphorylated T308 Resists Dephosphorylation by Interacting with H194 and R273 Residues. Analysis of the three-dimensional struc-

tures of Akt bound to either ATP or A-443654 (18, 19) suggested the possibility that the phosphorylated T308 interacts with H194 and R273 of the nucleotide-binding pocket (Fig. 4*A*, Fig. S3*B*) and that these intramolecular, ATP binding-dependent interactions could shield pT308 from phosphatase attack. To test this hypothesis, we mutated either H194 or R273 in MyrAkt1 to alanine. Cells expressing these mutants revealed markedly reduced steady-state T308 phosphorylation levels whereas inhibiting cellular phosphatases with calyculin restored high levels of T308 and S473 phosphorylation to the H194A and R273A mutants (Fig. 4*B*). These results are consistent with the notion that these mutations primarily enhanced Akt dephosphorylation. Next, we isolated the R273A mutant protein by immunprecipitation and found that when MyrAkt1 or WT-Akt1 R273 sites were mutated to alanine, neither ATP nor nonhydrolyzable ATP-γS were able to

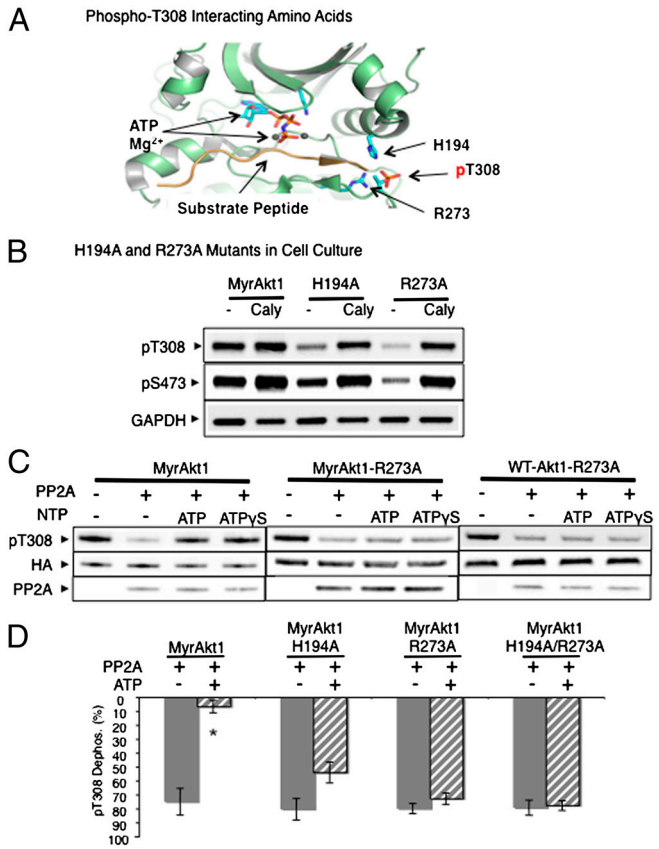

Fig. 4. Mutating Akt1 H194 and R273 abolishes ATP-mediated dephosporylation resistance. (*A*) Schematic view of the Akt1 catalytic cleft showing the nucleotide-binding pocket with bound ATP and Mg^{2+} and phosphorylated T308 interacting with H194 and R273 (19). The structure shown is modeled on active human Akt2 crystal structures bound to ATP analog AMP-PNP and Mn^{2+} (PDB 1o6k). However, we denoted ATP and Mg^{2+} and corresponding Akt1 amino acid residues for clarity. (*B*) MyrAkt1 H194A and R273A mutants were transfected into Hela cells. After 48 h, cells were propagated for four additional hours in exogenous growth factor-free medium followed by adding calyculin phosphatase inhibitor for 15 min. Akt T308 and S473 phosphorylation and HA-tag was analyzed by immunoblotting. (*C*) R273A mutation in WT Akt1 and in MyrAkt1 abolished ATP-mediated dephosphorylation resistance. Prephosphorylated MyrAkt1, MyrAkt1-R273A, or WT-Akt1-R273A were immunoprecipitated and incubated with recombinant PP2A in the presence of 100 uM ATP or 100 uM ATPγS for 30 min, 30 °C. Akt expression, T308 phosphorylation, and PP2A-C expression were analyzed by immunoblotting. (*D*) Quantification of T308 phosphorylation in MyrAkt1 mutants after PP2A treatment. Graph shows the percentage pT308 dephosphorylation by PP2A normalized to total Akt expression (Dephos. %) for MyrAkt ($n = 5$–7), H194A mutant ($n = 3$), R273A mutant ($n = 6$), and H194A/R273A mutant ($n = 2$–3). *$P < 0.001$ vs. PP2A for MyrAkt group. Not significant differences for H194A, R273A and H194A/R273A groups.

inhibit T308 dephosphorylation (Fig. 4*C*). Finally, mutating either H194 or R273 was sufficient to abolish ATP-mediated dephosphorylation resistance (Fig. 4*D*). These results support the hypothesis that molecular interactions of pT308 with H194 and R273 restrain PP2A access to this residue.

We noted that the phosphorylated S473 residue resists dephosphorylation with kinetics similar to those observed for phosphorylated T308 (Fig. 1*C*, 2*C*, and 4*B*). Furthermore, the crystal structure of active Akt with phosphorylated T308 and phosphomimetic S473 (PDB 1o6k) shows that the Akt carboxyl-terminal tail containing the phosphorylated S473 residue inserts into a hydrophobic groove in the N-lobe of Akt kinase (see Fig. S4*A* and ref. 19). In this stable conformation, Q218 contacts the phosphate group of phosphorylated S473 and the adjacent conserved tyrosine (Y474) makes hydrophobic contact with L213. To test whether these interactions could shield pS473 from phosphatase attack, we mutated Q218 and L213 in MyrAkt1 to alanine. Cells expressing these mutants revealed a markedly reduced steady-state Akt phosphorylation, while inhibiting cellular phosphatases with calyculin restored phosphorylation in the mutants (Fig. S4*B*). Collectively, these results suggest that molecular interactions of both, T308 and S473 with residues in the catalytic cleft interfere with Akt dephosphorylation at either residue.

Molecular Dynamics (MD) Simulations of H194/pT308 Interactions with Bound ATP and Bound ADP. As ADP was markedly less effective at inhibiting Akt dephosphorylation by PP2A in vitro when compared to ATP (Fig. 3*A*), we performed all-atom molecular modeling and MD simulations to investigate the stability of ATP/ADP-induced conformations as they relate to H194 and pT308 interactions (Fig. 5*A*). In the ATP bound conformation, H194 and pT308 were in close contact and stabilized by a hydrogen bond from the E2 hydrogen to the phosphate oxygen (atom HE2 and phosphate O distance $= 2.7 \pm 0.1$ Å). In contrast, in the ADP bound conformation, the ATP binding pocket was more open resulting in an increased distance between H194 and pT308 (atom HE2 and phosphate O distance $= 8.9 \pm 0.1$ Å). The H194/pT308 interaction was consistently more stable in the ATP bound state than in the ADP bound state in MD simulations with or without the two catalytic Mg^{2+} ions. These observations suggested that conformational change in the H194/pT308 interaction upon ATP hydrolysis directly contributes to greater solvent exposure of the pT308 phosphate, and consequently less protection of dephosphorylation by ADP.

Human Akt2 with R274H Mutation Decreased Cell Viability and Failed to Resist Dephosphorylation in the Presence of ATP. A missense mutation of Akt2 R274, homologous to R273 of Akt1, has been observed in a family affected by autosomal-dominant diabetes mellitus and the R274H mutant dominantly inhibited Akt1 and Akt2 signaling (4). Consistent with these observations, transient overexpression of Akt1-R273A or Akt2-R274H mutants in H9C2 cells significantly reduced cell viability (Fig. S5). To ascertain whether the interaction between Akt2-R274 and the Akt2 activation loop (T309 in Akt2) would affect dephosphorylation of Akt2-T309, we mutated MyrAkt2 R274 to histidine (R274H). As expected, this mutation markedly reduced steady-state T309 phosphorylation, whereas the phosphatase inhibitor calyculin, preserved T309 phosphorylation (Fig. 5*B*). We then immunoprecipitated phosphorylated MyrAkt2 and MyrAkt2 R274H and incubated the immunoprecipitated Akt2 protein with PP2A in the presence of ATP or ATP-γS. While both ATP and ATP-γS effectively counteracted MyrAkt2 dephosphorylation, neither nucleotide inhibited dephosphorylation of the R274H mutant (Fig. 5*C*). Of note, George, et al. (4) also found that R274H AKT2 is catalytically inactive and that the Akt1 R273A mutant also failed to phosphorylate the recombinant GSK3 peptide in vitro (Fig. S6*A*). These results assign a previously unappreciated

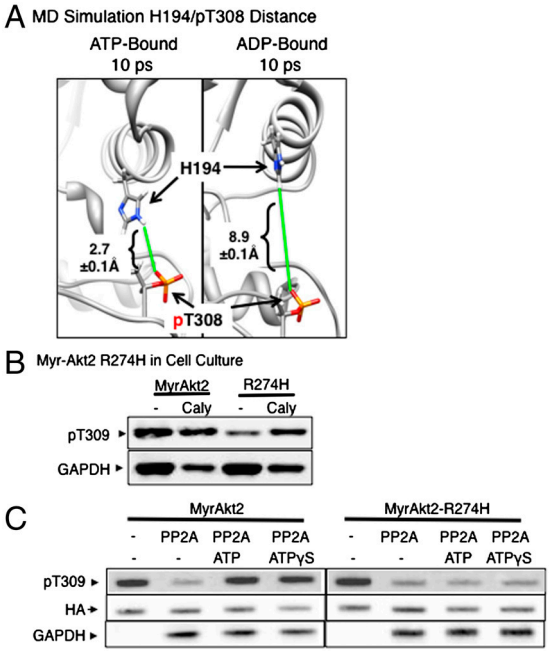

Fig. 5. (*A*) MD simulations compared the differences in the dynamics of the ATP and ADP bound Akt conformations and followed changes in H194 and pT308 interactions. The ATP and ADP complexes with Mg^{2+} ions were modeled into the crystal structure of AKT kinase bound to AMP-PNP (1o6 k). H194 and pT308 interactions were measured by the distance of a hydrogen bond from the E2 hydrogen to the phosphate oxygen. The first 1 ps of the simulation was for equilibration and the ensemble average distance was calculated over 1–10 ps. Images show modeled H194 to pT308 distance at 10 ps (green lines). (*B*) An Akt2 mutation (R274H) associated with human diabetes type II abolishes ATP-mediated dephosporylation resistance. MyrAkt2-R274H was transfected into Hela cells. After 48 h, cells were propagated for four additional hours in growth factor-free medium followed by adding 50 nM calyculin to inhibit cellular phosphatases for 15 min. Cell extracts were analyzed for Akt T309 phosphorylation and GAPDH by immunoblotting. (*C*) MyrAkt2 R274H mutant fails to resist dephosphorylation in the presence of ATP or ATPγS. Prephosphorylated MyrAkt2 or R274H mutant proteins were incubated with recombinant PP2A in the presence of 100 uM ATP or 100 uM ATPγS for 30 min, 30 °C. Akt expression and phosphorylation and PP2A-C expression were analyzed by immunoblotting.

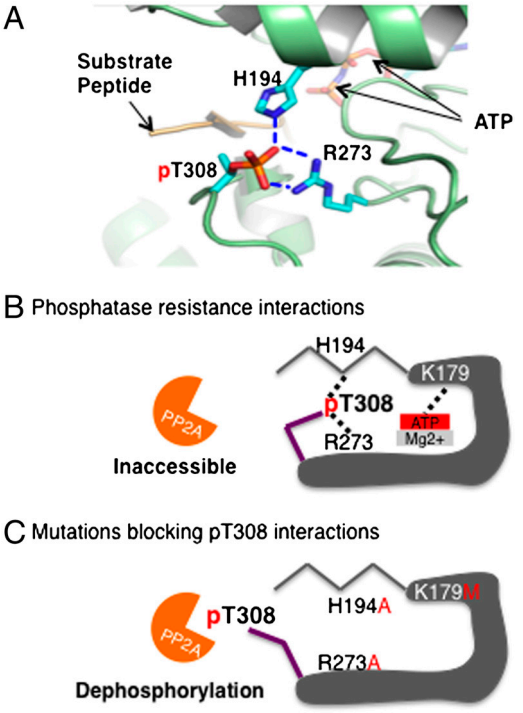

Fig. 6. The "Phosphatase Shielding Cage" induced by ATP binding of Akt. (*A*) Structural representation of the closed Akt activation loop conformation in the presence of substrate peptide and ATP. Under these conditions phosphorylated T308 is stabilized by H194 and R273 interactions. The structure is modeled on active human Akt2 crystal structures bound to ATP analog AMP-PNP and Mn^{2+} (PDB 1o6k). However, we indicated ATP and Mg^{2+} and corresponding Akt1 amino acid residues for clarity. (*B*) Stable interactions with H194 and R273 prevent access of phosphatases to phosphorylated T308. (*C*) Abolishing either pT308 interactions (H194A and R273A) or ATP binding (K179M) renders pT308 sensitive to phosphatase attack.

functional role to the R274H mutation related to T308 phophorylation and of potential relevance to the development of diabetes.

Discussion

The present study sheds light on a unique molecular mechanism regulating phosphorylation states of Akt1 and Akt2 through binding of either ATP or ATP-competitive antagonists. The most salient findings of this study can be summarized as follows: (*i*) binding of ATP or ATP-competitive antagonists to Akt1 restrained PP2A-mediated Akt1 dephosphorylation; and (*ii*) these effects were contingent on intramolecular interactions of phosphorylated T308 with H194 and R273 residues in the catalytic cleft of Akt1; (*iii*) steady-state Akt2 phosphorylation is similarly regulated by intramolecular interactions between T309 and R274. The interactions between phosphorylated T308 and residues in the catalytic cleft of Akt1 may restrict access of phosphatases to phosphorylated T308, thus providing a "molecular cage" to shield phosphorylated T308 from dephosphorylation (schematically depicted in Fig. 6*A*).

Docking of ATP to the ATP acceptor site of Akt1 not only enables phosphate transfer but also induces conformational changes in the Akt kinase domain (19). This effect is likely to contribute to the formation of a molecular cage that shields phosphorylated T308 from phosphatase attack. The catalytic domain of protein kinases, highly homologous among serine/threonine and tyrosine kinases, is composed of two subdomains, the beta sheet-rich N-lobe and the α-helix-rich C-lobe (19, 20). In the absence of ATP, the Akt catalytic domain remains in an open conformation and both, the activation loop containing T308 and the hydrophobic motif tail containing S473 are disordered (21). In this disordered state, the phosphorylated T308 and S473 can readily be accessed by phosphatases, such as PP2A. Upon coordinated binding of ATP/Mg^{2+} and substrate peptides at the interface between the N-lobe and C-lobe (19), both the activation loop containing phosphorylated T308 and phosphorylated S473 tail segment transition from the disordered "open" conformation to a more stable "closed" conformation (19). The "closed" conformation is stabilized by a network of residues that engage the phosphate groups of either phosphorylated T308 or S473 (Fig. 6*A*, Fig. S4*A*). The data presented here are fully compatible with this model and suggest that the closed conformation of the N- and C-lobes holds both phosphorylated T308 and phosphorylated S473 in a position that restrains phosphatase access and/or activity (Fig. 6*B*, Fig. S4*A*).

This conclusion is further supported by the finding that phosphorylated T308 in the activation loop becomes more susceptible to phosphatase attack when the closed conformation is weakened, either by excluding ATP/Mg^{2+} or substrate, or by introducing mutations in residues (H194A or R273A) that directly contact pT308 in the closed state (Fig. 6*C*). Interestingly, A446534 alone appears capable of supporting the closed, phosphatase-resistant conformation of Akt, even when H194 and R273 are mutated to alanine (Fig. S6*B*), suggesting that this compound forms additional, strong contacts with both lobes of the catalytic cleft thus robustly holding Akt in the closed, phosphatase-resistant state. Consistent with this

conclusion, A-443654 binds to several residues in the ATP binding pocket (G234 and M281) in addition to K179 (18).

The mechanisms described here may apply generally to ATP-competitive inhibitors of Akt1. Specifically, two structurally distinct ATP-competitive Akt inhibitors, (A-443654 and GSK-690693), induce Akt hyperphosphorylation (15, 16, 22, 23). Okuzumi and colleagues used cellular-based chemical genetics studies to show that binding of synthetic chemicals to the ATP binding site can induce Akt hyperphosphorylation (17). However, this approach did not reveal whether drug-induced hyperphosphorylation was due to excess phosphorylation or due to reduced dephosphorylation or both. Perhaps of equal importance, the approach taken by Okuzumi, et al. did not interrogate the functional consequences of the binding of natural nucleotides such as ATP and ADP to the Akt kinase domain. By contrast, the in vitro reconstitution assays introduced in the present study together with extensive cell-based biochemical evidence, directly speaks to the functional consequences of natural substrate (ATP) binding to the Akt kinase domain beyond the phosphate donor function. In essence, the novelty of our contribution lies in demonstrating that restraining phosphatase access by conformational, activation-dependent mechanisms is essential in understanding Akt hyperphosphorylation due to ATP binding site occupancy.

Please note that A-443654 efficiently blocked phospho-Akt immobilized with anti-HA-beads yet failed to block dephoshorylation of solubilized phospho-Akt (Fig. S6*C*). This result is consistent with the view that intracellular conditions, in particular anchoring at membrane-proximal vs. cytosolic compartments may impose constraints on ATP loading and/or conformation. Most of our results were generated using membrane-proximal MyrAkt1 of relevance to neoplasia harboring mutations driving hyperactivation (and membrane translocation) of Akt. Furthermore, in contrast to ATP, the A-443654 compound cannot be hydrolyzed and, for that reason, may be expected to reside in the ATP binding pocket for considerably longer periods of time. This hydrolysis of ATP may explain why the ATP concentration (1 mM) required for dephosphorylation resistance was considerably higher than that of A-443654 (2–10 uM) required for this effect (Fig. S3*A*). This view is further supported by our experiments demonstrating that blocking Akt ATP hydrolysis with a high affinity pseudosubstrate peptide inhibitor (I-T15A, VELDPEFEPRARERAYAFGH) lowers the ATP concentration required to inhibit Akt dephoshorylation (Fig. 2*C*, Fig. S3*A*). Collectively, these data suggested that sustained occupation of ATP acceptor site with either ATP or ATP-competitive inhibitor is subject to multiple levels of stringent regulation beyond the ATP abundance in the cytosol.

The active conformation of Akt kinase is highly homologous to the active conformations of other protein kinases. Of particular relevance to the findings reported here, phosphorylation of residues within centrally located "activation loops" is frequently required for catalysis (19, 20). Similar to inhibitors of Akt kinase, inhibitors that occupy the nucleotide-binding pocket of other protein kinases also induce hyperphosphorylation of serine/threonine residues in activation loops. For example, hyperphosphorylation of the Map2k MEK occurs upon exposure to many MEK inhibitors, including U0126, PD098059, and PD184161, Cl-1040, and AZD6244 (24–26). While these inhibitors are all allosteric and non-ATP-competitive, they all bind to a hydrophobic pocket adjacent to the ATP binding site (27). ATP binding similarly controls activation loop phosphorylation of PKC (28, 29). Thus, most likely, intrinsic binding of ATP also shields phosphorylated MEK and PKC from dephosphorylation by phosphatases. Of note, we took account of and confirmed a previous report (30) that the inclusion of Mg^{2+} and Mn^{2+} divalent metal ions in the reaction mixture abrogates inhibition of PP2A catalytic activity by nonspecific negative ion effects of ATP, GTP, and sugar phosphates (Fig. S6*D*).

Collectively, the results of the present study point to a general autoregulatory mechanism shared among diverse protein kinases that relates to conformational changes of the activation domain induced by ATP binding. This mechanism serves to facilitate interaction of phosphorylated residues in the activation loop with residues in the catalytic fold and renders them resistant to ambient phosphatases. At least one of those residues (R274 in Akt2) has been linked to a disease state in humans (4). A family of patients with severe insulin resistance was found to carry a heterozygous loss-of function mutation in Akt2 (R274H) (4). Not only does the R274H mutation render Akt2 catalytically inactive, but the R274H mutant also acts as dominant-negative to block adipocyte differentiation and more directly, block the ability of WT Akt1 and Akt2 to inhibit the Akt-dependent transcriptional activity of FOXA2. Furthermore, Kitamura, et al. (32) have shown that Akt carrying mutations at both regulatory phosphorylation sites (T308 and S473 to alanine, AA mutant) dominantly inhibits insulin activation of WT-Akt in CHO cells. Because other catalytically inactive Akt mutants do not have significant dominant-negative properties (31, 32), it remains unresolved how the Akt2 R274H mutant interferes with WT Akt1 and Akt2 activities.

Our MD stimulation results suggested that the primary reason for ATP, but not ADP, to be protective of Akt dephosphorylation is likely due to the greater conformational flexibility of the ADP bound state when compared to the rigid ATP bound state. Consistently, previous molecular dynamics simulations of transition state mimetics (and with ATP) have demonstrated that the ATP bound state, but not the ADP bound state, exhibits exceptional stability at physiological temperature, suggesting the conformational fluctuation may contribute to the rate-limiting product release step of the bound ADP and Mg^{2+} ions (33–35). Molecules that bind Akt, but fail to protect Akt dephosphorylation will likely adopt conformation similar to ADP. On the other hand, the dephosphorylation protective crystal structure of AKT bound to A-443654 (PDB2jdr) is nearly identical to the AMP-PNP bound conformation (PDB1o6k).

In summary, the data presented here provide an explanation for the paradoxical hyperphosphorylation of the activation domains of kinases associated with the use of ATP-competitive inhibitors. Finally, the identification of multiple amino acid residues participating in this process and not conserved between kinases provides opportunities for the rational design of non-ATP-competitive kinase inhibitors for discrimination within and between protein kinase families.

Materials and Methods

Plasmids. AKT1 and Akt2 were fused at the amino-terminus with Src myristoylation signal (Myr) and at the carboxyl-terminus with Hemagglutinin epitope (HA). All mutant constructs were generated using standard molecular biology strategies and were confirmed by DNA sequencing in the core facilities of Kimmel Cancer Center. HA-epitope-tagged PRAS40 in pRK5 expression vector was from Addgene (#15481). Detailed methods are located in the *SI Text*.

Chemicals. ATP and ATP analogs were purchased from Sigma. Per-VO4 was prepared fresh by mixing equal molar amounts of hydrogen peroxide and NaVO4 (36). Akt-specific substrate peptide (37), RPRAATF, was from Millipore. High affinity I-T15A Akt pseudo substrate peptide, derived from the fusion between an Akt peptide substrate (AKTide-2T) and an Akt substrate peptide from FOXO3 gene (38), (VELDPEFEPRARERAYAFGH), were synthesized by Genscript. Inhibitors were used on cell culture in the following concentrations: 200 nM wortmannin (PI-3 kinase inhibitor, EMD Chemicals), 0.5 uM UCN01 [PDK1 inhibitor (39), EMD Chemicals], 10 uM VIII [allosteric Akt inhibitor (11, 12), EMD Chemicals], 10 uM A-443654 [ATP-competitive Akt inhibitor (22), Abbott Laboratories], 100 nM Calyculin A (phosphatase inhibitor, Cell Sign. Tech.) and 250 nM okadiac acid (phosphatase inhibitor, EMD Chemicals).

Cell Culture and Transfection. H9C2 cells derived from rat neonatal hearts (ATCC) were cultured in M199 medium supplemented with 10% fetal calf

serum and antibiotics. Human epitheloid carcinoma-derived Hela cells were cultured in Dulbecco's Modified Eagle's Essential Medium (DMEM) supplemented with 10% fetal calf serum and antibiotics. Cells were transfected using Fugene-6 HD (Roche) according to the manufacturer's protocols.

In Culture Akt Dephosphorylation. To maximally activate endogenous Akt, H9C2 cells were serum-starved for 4 h before stimulating with 1 ug/mL insulin for 20 min. To initiate dephosphorylation, insulin medium was replaced with serum-free medium in the presence of indicated inhibitors. After 10 min of incubation, cells were harvested for immunoblotting analysis.

Cell Extract Akt Dephosphorylation. Human epitheloid carcinoma-derived Hela cells were treated with Per-VO4 (15 min, 100 uM hydrogen peroxide and 100 uM sodium orthovanadate) to maximally activate Akt. The same experiments were performed using serum-starved H9C2 cells stimulated with 1 ug/mL insulin for 20 min. To harvest, stimulated cells were washed once with ice-cold PBS before placing cell culture dish on an ethanol/dry ice bath to flash freeze. Cell-free extracts were prepared by scraping flash-frozen cells into Phosphatase Assay Buffer (50 mM Hepes, pH 7.5, 100 mM NaCl, 1 mM EDTA, 1 mM EGTA 10 mM NaF supplemented with 5 μg/mL leupeptin, 5 μg/mL aprotinin, 10 mM PMSF, and 1 mM DTT) and then, douncing the extracts with fitted plastic pestle on ice. Total cell-free extracts were incubated at 30 °C to initiate dephosphorylation. At the indicated times, a fixed amount of cell extract was removed from incubation and dephosphorylation stopped by adding equal volume of Stop Assay Buffer (25 mM Tris-HCl pH 7.6, 137 mM NaCl, 10% glycerol, 1% NP40, 10 mM NaF supplemented with 5 μg/mL leupeptin, 5 μg/mL aprotinin, 10 mM PMSF, 1 mM NaVO4 and 100 nM Calyculin, 20 mM β-glycerolphosphate and 1 mM Sodium pyrophosphate). After lysis on ice for 10–20 min, phosphatase-inhibited cell lysates was clarified, reduced, and denatured by PAGE sample buffer for immunoblotting.

In Vitro Akt Dephosphorylation by Phosphatase 2A (PP2A). Immunopurified Akt was dephosphorylated in vitro using recombinant PP2A catalytic subunit (PP2A-C). Briefly, Hela cells overexpressing HA-tagged and constitutively phosphorylated Myr-Akt1 were lysed in NP40 lysis buffer (25 mM Tris-HCl pH 7.6, 137 mM NaCl, 10% glycerol, 1% NP40, 10 mM NaF) freshly supplemented with 1 mM Sodium pyrophosphate, 5 μg/mL leupeptin, 5 μg/mL aprotinin, 50 nM Calyculin, 1 mM EDTA, 10 mM PMSF,1 mM NaVO4 and 1 mM DTT. For immunoprecipitation, clarified cellular lysates were diluted with equal volume of Phosphatase Assay Buffer (50 mM Hepes, pH 7.5, 100 mM NaCl, 1 mM EDTA, 1 mM EGTA 10 mM NaF supplemented with 5 μg/mL leupeptin, 5 μg/mL aprotinin, 10 mM PMSF, and 1 mM DTT). HA-tagged Myr-Akt was immuno-purified by incubation with anti-HA agarose affinity gel (Sigma) for 3 h at 4 °C. The immunoprecipitates were washed sequentially at 4°C, 3× with equal mix of NP40 lysis buffer and Phosphatase Assay Buffer, then, 3x Phosphatase Assay Buffer. After washing, immunoprecipitates were aliquoted and added inhibitors and ATP analogs as indicated at 4 °C. Dephosphorylation was conducted in Phosphatase Assay Buffer (50 uL final volume, supplemented with 5 mM MgCl2, 30 °C for the indicated times) containing 40 ng recombinant PP2A catalytic subunit (WT or L309 deletion, Cayman Chemicals) and 40 uM 1,2-Dipalmitoyl-*sn*-glycero-3-phosphoserine and 40 uM 1,2-Dipalmitoyl-*sn*-glycero-3-phosphocholine (Echelon Biosciences). After indicated incubation time, assay was stopped by PAGE sample buffer and analyzed for Akt T308 and Akt S473 phosphorylation as well as total Akt and PP2A-C expression.

Immunoblotting. Akt kinase assay and Akt phosphorylation (S473 and T308) were visualized and directly quantified using the Odyssey Infrared Imaging System (Li-Cor) as described previously (40). Detailed methods are located in *SI Text*. The following antibodies were used at 1 : 1,000 dilution: antiphospho-GSK3 (Ser21/9), antiphospho-Pras40 (Ser246), antitotal Akt, anti-phospho-Akt (T308), antiphospho-Akt (S473), anti-GAPDH (from Santa Cruz) and anti-HA (from Covance).

Immunofluorescence Microscopy. Immunofluorescence microscopy procedures and image acquisition were performed as previously described (41). Detailed methods are located in the *SI Text*. MD stimulation. The program CHARMM (Chemistry at Harvard Molecular Mechanics) was used for all-atom modeling and MD (42). Detailed methods are located in the *SI Text*.

Statistical Analysis. A commercial software package was used for statistical analysis (Graph Pad Software Inc). Comparison of means ± SE was analyzed by nonparametric Mann-Whitney test or nonparametric ANOVA (Kruskal-Wallis with Dunn posttest).

ACKNOWLEDGMENTS. This work was supported by the National Heart, Lung, and Blood Institute grant HL 091799-01 (A.M.F.), HL 58672, HL 74854 (J.Y.C.), the American College of Radiology and the Commonwealth of Pennsylvania (U.R.) and American Heart Association SDG F64701 (T.O.C).

1. Chan TO, Rittenhouse SE, Tsichlis PN (1999) AKT/PKB and other D3 phosphoinositide-regulated kinases: kinase acvtivation by phosphoinositide-dependent phosphorylation. *Ann Rev Biochem* 68:965–1015.
2. Fayard E, Xue G, Parcellier A, Bozulic L, Hemmings BA (2010) Protein kinase B (PKB/Akt), a key mediator of the PI3K signaling pathway. *Curr Top Microbiol Immunol* 346:31–56.
3. Dummler B, Hemmings BA (2007) Physiological roles of PKB/Akt isoforms in development and disease. *Biochem Soc Trans* 35:231–235.
4. George S, et al. (2004) A family with severe insulin resistance and diabetes due to a mutation in AKT2. *Science* 304:1325–1328.
5. Andjelkovic M, et al. (1996) Activation and phosphorylation of a pleckstrin homology domain containing protein kinase (RAC-PK/PKB) promoted by serum and protein phosphatase inhibitors. *Proc Natl Acad Sci USA* 93:5699–5704.
6. Resjo S, et al. (2002) Protein phosphatase 2 A is the main phosphatase involved in the regulation of protein kinase B in rat adipocytes. *Cell Signal* 14:231–238.
7. Kuo YC, et al. (2008) Regulation of phosphorylation of Thr-308 of Akt, cell proliferation, and survival by the B55alpha regulatory subunit targeting of the protein phosphatase 2 A holoenzyme to Akt. *J Biol Chem* 283:1882–1892.
8. Vereshchagina N, Ramel MC, Bitoun E, Wilson C (2008) The protein phosphatase PP2A-B' subunit Widerborst is a negative regulator of cytoplasmic activated Akt and lipid metabolism in Drosophila. *J Cell Sci* 121:3383–3392.
9. Padmanabhan S, et al. (2009) A PP2A regulatory subunit regulates *C. elegans* insulin/IGF-1 signaling by modulating AKT-1 phosphorylation. *Cell* 136:939–951.
10. Hanada M, Feng J, Hemmings BA (2004) Structure, regulation and function of PKB/AKT–a major therapeutic target. *Biochim Biophys Acta* 1697:3–16.
11. Barnett SF, et al. (2005) Identification and characterization of pleckstrin-homology-domain-dependent and isoenzyme-specific Akt inhibitors. *Biochem J* 385:399–408.
12. Logie L, et al. (2007) Characterization of a protein kinase B inhibitor in vitro and in insulin-treated liver cells. *Diabetes* 56:2218–2227.
13. Calleja V, Laguerre M, Parker PJ, Larijani B (2009) Role of a novel PH-kinase domain interface in PKB/Akt regulation: structural mechanism for allosteric inhibition. *PLoS Biol* 7:e17.
14. Wu WI, et al. (2010) Crystal structure of human AKT1 with an allosteric inhibitor reveals a new mode of kinase inhibition. *PLoS One* 5:e12913.
15. Han EK, et al. (2007) Akt inhibitor A-443654 induces rapid Akt Ser-473 phosphorylation independent of mTORC1 inhibition. *Oncogene* 26:5655–5661.
16. Levy DS, Kahana JA, Kumar R (2009) AKT inhibitor, GSK690693, induces growth inhibition and apoptosis in acute lymphoblastic leukemia cell lines. *Blood* 113:1723–1729.
17. Okuzumi T, et al. (2009) Inhibitor hijacking of Akt activation. *Nat Chem Biol* 5:484–493.
18. Davies TG, et al. (2007) A structural comparison of inhibitor binding to PKB, PKA and PKA-PKB chimera. *J Mol Biol* 367:882–894.
19. Yang J, et al. (2002) Crystal structure of an activated Akt/protein kinase B ternary complex with GSK3-peptide and AMP-PNP. *Nat Struct Biol* 9:940–944.
20. Huse M, Kuriyan J (2002) The conformational plasticity of protein kinases. *Cell* 109:275–282.
21. Yang J, et al. (2002) Molecular mechanism for the regulation of protein kinase B/Akt by hydrophobic motif phosphorylation. *Mol Cell* 9:1227–1240.
22. Luo Y, et al. (2005) Potent and selective inhibitors of Akt kinases slow the progress of tumors in vivo. *Mol Cancer Ther* 4:977–986.
23. Rhodes N, et al. (2008) Characterization of an Akt kinase inhibitor with potent pharmacodynamic and antitumor activity. *Cancer Res* 68:2366–2374.
24. Wang Y, et al. (2005) A role for K-ras in conferring resistance to the MEK inhibitor, CI-1040. *Neoplasia* 7:336–347.
25. Huynh H, Soo KC, Chow PK, Tran E (2007) Targeted inhibition of the extracellular signal-regulated kinase kinase pathway with AZD6244 (ARRY-142886) in the treatment of hepatocellular carcinoma. *Mol Cancer Ther* 6:138–146.
26. Yip-Schneider MT, et al. (2009) Resistance to mitogen-activated protein kinase kinase (MEK) inhibitors correlates with up-regulation of the MEK/extracellular signal-regulated kinase pathway in hepatocellular carcinoma cells. *J Pharmacol Exp Ther* 329:1063–1070.
27. Ohren JF, et al. (2004) Structures of human MAP kinase kinase 1 (MEK1) and MEK2 describe novel noncompetitive kinase inhibition. *Nat Struct Mol Biol* 11:1192–1197.
28. Cameron AJ, Escribano C, Saurin AT, Kostelecky B, Parker PJ (2009) PKC maturation is promoted by nucleotide pocket occupation independently of intrinsic kinase activity. *Nat Struct Mol Biol* 16:624–630.
29. Srivastava J, Goris J, Dilworth SM, Parker PJ (2002) Dephosphorylation of PKCdelta by protein phosphatase 2Ac and its inhibition by nucleotides. *FEBS Lett* 516:265–269.
30. Kowluru A, Metz SA (1998) Purine nucleotide- and sugar phosphate-induced inhibition of the carboxyl methylation and catalysis of protein phosphatase-2A in insulin-secreting cells: protection by divalent cations. *Biosci Rep* 18:171–186.
31. van Weeren PC, de Bruyn KM, de Vries-Smits AM, van Lint J, Burgering BM (1998) Essential role for protein kinase B (PKB) in insulin-induced glycogen synthase kinase

3 inactivation. Characterization of dominant-negative mutant of PKB. *J Biol Chem* 273:13150–13156.
32. Kitamura T, et al. (1998) Requirement for activation of the serine-threonine kinase Akt (protein kinase B) in insulin stimulation of protein synthesis but not of glucose transport. *Mol Cell Biol* 18:3708–3717.
33. Bao ZQ, Jacobsen DM, Young MA (2011) Briefly bound to activate: transient binding of a second catalytic magnesium activates the structure and dynamics of CDK2 kinase for catalysis. *Structure* 19:675–690.
34. Khavrutskii IV, Grant B, Taylor SS, McCammon JA (2009) A transition path ensemble study reveals a linchpin role for $Mg^{(2+)}$ during rate-limiting ADP release from protein kinase A. *Biochemistry* 48:11532–11545.
35. Zimmermann B, Schweinsberg S, Drewianka S, Herberg FW (2008) Effect of metal ions on high-affinity binding of pseudosubstrate inhibitors to PKA. *Biochem J* 413:93–101.
36. Bennett PA, Dixon RJ, Kellie S (1993) The phosphotyrosine phosphatase inhibitor vanadyl hydroperoxide induces morphological alterations, cytoskeletal rearrangements and increased adhesiveness in rat neutrophil leucocytes. *J Cell Sci* 106:891–901.
37. Bozinovski S, Cristiano BE, Marmy-Conus N, Pearson RB (2002) The synthetic peptide RPRAATF allows specific assay of Akt activity in cell lysates. *Anal Biochem* 305:32–39.
38. Luo Y, et al. (2004) Pseudosubstrate peptides inhibit Akt and induce cell growth inhibition. *Biochemistry* 43:1254–1263.
39. Sato S, Fujita N, Tsuruo T (2002) Interference with PDK1-Akt survival signaling pathway by UCN-01 (7-hydroxystaurosporine). *Oncogene* 21:1727–1738.
40. Chan TO, et al. (2002) Small GTPases and tyrosine kinases coregulate a molecular switch in the phosphoinositide 3-kinase regulatory subunit. *Cancer Cell* 1:181–191.
41. Chan TO HF, et al. (2008) Cardiac-restricted overexpression of the A_{2A}-adenosine receptor in FVB Mice transiently increases contractile performance and rescues the heart failure phenotype in mice overexpressing the A_1-adenosine receptor. *Clinical and Translational Science* 1:126–133.
42. Brooks BR, et al. (2009) CHARMM: the biomolecular simulation program. *J Comput Chem* 30:1545–1614.